21st Annual Conference of the Canadian Nuclear Society
Toronto, Ontario, Canada / June 11 - 14, 2000

# Application of Non-Linear Iterative Nodal Expansion Method for CANDU Analysis (Part I: Derivation of the Steady-State Nodal Diffusion Formulation)

Wei Shen
Atomic Energy of Canada Limited
2251 Speakman Drive
Mississauga, Ontario L5K 1B2

Hangbok Choi
Korea Atomic Energy Research Institute
P.O. Box 105, Yusong
Taejon, 305-600, Korea

## ABSTRACT

*The steady-state nodal diffusion formulation of the non-linear iterative nodal expansion method (NEM) is derived independently and is illustrated in detail in this paper. A simple two-dimensional two-group diffusion code with the capability of both finite-difference method (FDM) and NEM techniques is also developed. The preliminary numerical tests show that the formulation derived in the paper is correct, and the NEM always shows superior accuracy over the FDM for a given mesh design, even for CANDU® analysis. The coarse-mesh (about 20-cm mesh spacing for a pressurized-water reactor (PWR) and 30-cm mesh spacing for a CANDU reactor) NEM results are as accurate as the fine-mesh (about a 1- to 1.5-cm mesh spacing for PWR, and a 5-cm mesh spacing for a CANDU reactor) FDM results for both PWR and CANDU analysis.*

## 1. INTRODUCTION

The nodal method has been used for light-water reactor (LWR) core-physics and safety analysis for more than 20 years. However, because of the large migration area in heavy-water reactor systems, the coarse-mesh finite-difference method (FDM) has generally been found to be adequate and has been extensively used for CANDU analysis in the past three decades. To address the increased accuracy requirements of current and future analysis, the nodal method is being investigated as an alternative tool for CANDU analysis, especially for transient scenarios when the spatial flux changes rapidly.[1]

Among the numerous advanced nodal methods, the nodal expansion method (NEM)[2] has been preferred because of its rich history of success, adaptability, and popularity. The classical approach to NEM is the response-matrix formulation, as adopted in the Siemens PANBOX code[2] and the Westinghouse ANC code[3]. To minimize memory requirements, and especially to facilitate the capability of applying either the NEM or the FDM formulation within a single code, an alternative non-linear iterative approach to NEM is proposed in this study. This technique was originally developed by Smith[4], successfully implemented in the Studsvik Scandpower QPANDA[5] and SIMULATE-3[6] codes, and subsequently refined and extended in the FORMOSA[7] and NESTLE[8] codes.

The basic idea of the non-linear iterative NEM strategy is that, by correcting the FDM diffusion coupling

® CANDU is a registered trademark of Atomic Energy of Canada Limited (AECL).

coefficients periodically, it is possible for the FDM to reproduce exactly the same interface net currents as those computed by the NEM. Therefore, instead of iteratively solving the complex response-matrix NEM formulations, most of the computational effort may be shifted to the less-expensive solution of the FDM equations, in which node-average fluxes are the only unknowns. Compared with other nodal methods, the advantages of the non-linear iterative NEM strategy are obvious:

1) The simplicity of the algorithm and the ease of implementation. For a given FDM code such as the Reactor Fuelling Simulation Program (RFSP)[9], the finite-difference matrix system of equations and unknowns is left structurally intact. With a minor correction to the coupling coefficients in the current FDM code, the NEM can be implemented directly as an alternative option for the solution of the diffusion equation, while sharing the same geometry, cross sections, and iteration procedures as those of the FDM.
2) The reduced number of unknowns (node volume-average fluxes rather than surface-average currents are used as the unknowns).
3) The reduced storage requirements (two-node problem arrays are reusable at each nodal surface).

Although the non-linear iterative NEM strategy has been successfully used for LWR analysis, the documentation available on this technique is scarce because it was originally designed for commercial software. In this paper, the steady-state nodal diffusion formulation of the non-linear iterative NEM technique is derived independently and is illustrated in detail. A simple two-group diffusion code with the capability of both FDM and NEM techniques has been developed. Once it is proven to be an efficient method for CANDU analysis, it should be practical to implement this technique in a production code such as RFSP in the future.

## 2. FDM APPROXIMATION

By partitioning the Cartesian system into K homogeneous nodes $V^k$, k=1,2,… ,K, the G-group three-dimensional (3-D) steady-state neutron-diffusion equation is written in the standard form:

$$\sum_{u=x,y,z} \frac{\partial}{\partial u} J_{gu}^k(\vec{r}) + \Sigma_{rg}^k \phi_g^k(\vec{r}) = Q_g^k(\vec{r}) \tag{1a}$$

where

$$\vec{r} = (x,y,z);\ u = x,y,z;\ g = 1,...,G;\ k = 1,...,K$$

and

$$Q_g^k(\vec{r}) = \frac{\chi_g^k}{\lambda} \sum_{g'=1}^{G} (\nu\Sigma_f)_{g'}^k \phi_{g'}^k(\vec{r}) + \sum_{\substack{g'=1 \\ g' \neq g}}^{G} \Sigma_{gg'}^k \phi_{g'}^k(\vec{r}) \tag{1b}$$

By using Fick's Law, the u-direction net neutron current can be expressed as:

$$J_{gu}^k(\vec{r}) = -D_g^k \frac{\partial}{\partial u} \phi_g^k(\vec{r}) \tag{1c}$$

Integrating Equation (1) over spatial node $V^k$ with homogenized properties, and with half-widths $a_x^k$, $a_y^k$,

$a_z^k$, we obtain the well-known nodal balance equation, which we write in terms of the surface-average currents $J_{gu}^k(\pm a_u^k)$ as follows:

$$\sum_{u=x,y,z} 2a_v^k 2a_w^k \left[\bar{J}_{gu}^k(a_u^k) - \bar{J}_{gu}^k(-a_u^k)\right] + \Sigma_{r,g}^k \bar{\phi}_g^k V^k = \bar{Q}_g^k V^k \qquad (2a)$$

$$u,v,w = x,y,z;\ u \neq v \neq w;\ g = 1,\ldots,G;\ k = 1,\ldots,K$$

where the node volume-average flux and source are defined as:

$$\bar{\phi}_g^k = \frac{1}{V^k}\int_{-a_x^k}^{-a_x^k} dx \int_{-a_y^k}^{-a_y^k} dy \int_{-a_z^k}^{-a_z^k} \phi_g^k(\vec{r})\,dz \qquad (2b)$$

$$\begin{aligned}\bar{Q}_g^k &= \frac{1}{V^k}\int_{-a_x^k}^{-a_x^k} dx \int_{-a_y^k}^{-a_y^k} dy \int_{-a_z^k}^{-a_z^k} Q_g^k(\vec{r})\,dz \\ &= \frac{\chi_g^k}{\lambda}\sum_{g'=1}^{G}(\nu\Sigma_f)_{g'}^k \bar{\phi}_{g'}^k + \sum_{\substack{g'=1 \\ g'\neq g}}^{G}\Sigma_{gg'}^k \bar{\phi}_{g'}^k\end{aligned} \qquad (2c)$$

and $V^k = 2a_u^k\, 2a_v^k\, 2a_w^k$ represents the volume of node *k*.

The surface-average current over the node surface at $u = \pm a_u^k$, is given by:

$$\bar{J}_{gu}^k(\pm a_u^k) = \frac{1}{2a_v^k}\frac{1}{2a_w^k}\int_{-a_v^k}^{a_v^k} dv \int_{-a_w^k}^{a_w^k} dw J_{gu}^k(\pm a_u^k, v, w) \qquad (2d)$$

The solution of Equation (2a) requires additional equations relating the surface-average currents to the node volume-average fluxes. It is these additional coupling relationships that characterize the various schemes that have been developed for the solution of the neutron-diffusion equation. Certainly, one of the simplest means of obtaining these relationships is the well-known mesh-centred FDM approximation as adopted in the RFSP code, as explained below.

First, we consider (for simplicity) a two-dimensional (2-D) view of the nodal model in Figure 1, showing a central node labelled "0" and its closest neighbours labelled "*n*", *n* = 1 to 6 (with only *n* = 1 to 4 shown in the 2-D view). The surface-average current over the node 0 surface at $u = \pm a_u^0$, is expressed as a linear combination of the node volume-average fluxes in two adjacent nodes, respectively:

$$\bar{J}_{gu}^{0,FDM}(+a_u^0) = -\frac{d_g^{02,FDM}}{2a_v^0\, 2a_w^0}\left[\bar{\phi}_g^2 - \bar{\phi}_g^0\right] \qquad (3a)$$

$$\bar{J}_{gu}^{0,FDM}(-a_u^0) = -\frac{d_g^{01,FDM}}{2a_v^0\, 2a_w^0}\left[\bar{\phi}_g^0 - \bar{\phi}_g^1\right] \qquad (3b)$$

where the FDM diffusion coupling coefficients between node 0 and its neighbours *n*=1,2 are:

$$d_g^{0n,FDM} = 2a_v^0 2a_w^0 \Big/ \left( \frac{a_u^0}{D_g^0} + \frac{a_u^n}{D_g^n} \right), \quad n = 1, 2$$

The generalization to the coefficients $d_g^{0n,FDM}$ for any of the six interfaces $n$ is evident. Direct substitution of Equation (3) into Equation (2) results in the FDM neutron-diffusion equation with node volume-average fluxes as the spatial unknowns:

$$\sum_{n=1}^{6} d_g^{0n,FDM} \left( \bar{\phi}_g^0 - \bar{\phi}_g^n \right) + \Sigma_{r,g}^0 \bar{\phi}_g^0 V^0 = \bar{Q}_g^0 V^0 \tag{4}$$

This equation couples any node 0 to its six neighbours $n$, and through these, to all other nodes. Each term $d_g^{0n,FDM} \left( \bar{\phi}_g^0 - \bar{\phi}_g^n \right)$ represents the group-g leakage out of the node 0 across the surface with its neighbour node $n$. For the system with K homogeneous nodes by G-group approximation, the finite-difference form of the neutron-diffusion equation is then a coupled set of K x G linear homogeneous equations of type (4), which can be solved effectively. Unfortunately, Equation (3) corresponds to a first-order Taylor expansion with a large truncation error in a coarse-mesh application, which may translate into an inaccurate characterization of the interface-average currents and, hence, node volume-average flux.

## 3. NEM FORMULATION

The development of interface-current nodal methods such as the NEM is motivated by the need for improved accuracy relative to the FDM for a given mesh design. NEM chooses to treat the surface-average currents in Equation (2a) as additional unknowns, and these surface-average currents can be predicted accurately by solving the one-dimensional (1-D) transverse-integrated equations.

### 3.1 One-Dimensional Transverse-Integrated Equations

Integrating Equation (1) over the two directions transverse to each axis, we obtain three 1-D equations for the flux and current, one for each direction in Cartesian coordinates, of the following form:

$$\frac{\partial}{\partial u} \bar{J}_{gu}^k(u) + \Sigma_{rg}^k \phi_{gu}^k(u) = Q_{gu}^k(u) - \frac{1}{2a_v^k} L_{gv}^k(u) - \frac{1}{2a_w^k} L_{gw}^k(u) \tag{5a}$$

$$u = x, y, z; g = 1, \ldots, G; k = 1, \ldots, K$$

where the transverse-integrated flux and source are defined as:

$$\phi_{gu}^k(u) = \frac{1}{2a_v^k} \frac{1}{2a_w^k} \int_{-a_v^k}^{-a_v^k} dv \int_{-a_w^k}^{-a_w^k} dw \phi_g^k(u, v, w) \tag{5b}$$

$$Q_{gu}^k(u) = \frac{1}{2a_v^k} \frac{1}{2a_w^k} \int_{-a_v^k}^{-a_v^k} dv \int_{-a_w^k}^{-a_w^k} dw Q_g^k(u, v, w)$$

$$= \frac{\chi_g^k}{\lambda} \sum_{g'=1}^{G} (\nu\Sigma_f)_{g'}^k \phi_{g'u}^k(u) + \sum_{\substack{g'=1 \\ g' \neq g}}^{G} \Sigma_{gg'}^k \phi_{g'u}^k(u) \tag{5c}$$

the average u-directed transverse leakage along v and w, are given by:

$$L_{gv}^k(u) = \frac{1}{2a_w^k} \int_{-a_w^k}^{a_w^k} dw \left( J_{gv}^k(u, a_v^k, w) - J_{gv}^k(u, -a_v^k, w) \right) \tag{5d}$$

$$L_{gw}^k(u) = \frac{1}{2a_v^k} \int_{-a_v^k}^{a_v^k} dv \left( J_{gw}^k(u, v, a_w^k) - J_{gv}^k(u, v, -a_w^k) \right) \tag{5e}$$

the u-direction transverse-integrated current can be expressed as:

$$\bar{J}_{gu}^k(u) = \frac{1}{2a_v^k} \frac{1}{2a_w^k} \int_{-a_v^k}^{a_v^k} dv \int_{-a_w^k}^{a_w^k} dw J_{gu}^k(u, v, w) = -D_g^k \frac{\partial}{\partial u} \phi_{gu}^k(u) \tag{5f}$$

Note that, at the node surface $u = \pm a_u^k$, the u-direction transverse-integrated current defined in Equation (5f) is equivalent to the surface-average current defined in Equation (2d).

### 3.2 NEM Polynomial Approximation

The 1-D transverse-integrated nodal flux in Equation (5a) can be solved analytically. This results in the famous Analytic Nodal Method[1][10]. However, in the NEM, the 1-D transverse-integrated nodal flux is approximated by polynomials of the following form:

$$\phi_{gu}^k(u) = \bar{\phi}_g^k + \sum_{n=1}^{4} c_{gun}^k P_n(u) \tag{6a}$$
$$u = x, y, z; g = 1, \ldots, G; k = 1, \ldots, K$$

where $c_{gun}^k$ and $P_n(u)$ are the expansion coefficients and the basis functions, and $\bar{\phi}_g^k$ is the node volume-average flux. The accuracy of a nodal method depends on the selection of basis functions and the order N. For the quartic NEM, the following fourth-order basis functions are used:

$$P_1(u) = \xi; \tag{6b}$$

$$P_2(u) = 3\xi^2 - \frac{1}{4}; \tag{6c}$$

$$P_3(u) = \xi \left( \xi - \frac{1}{2} \right) \left( \xi + \frac{1}{2} \right); \tag{6d}$$

$$P_4(u) = \left( \xi^2 - \frac{1}{20} \right) \left( \xi - \frac{1}{2} \right) \left( \xi + \frac{1}{2} \right) \tag{6e}$$

where

$$\xi = \frac{u}{2a_u^k}; \quad -a_u^k \le u \le a_u^k \tag{6f}$$

$$\frac{1}{2a_u^k}\int_{-a_u^k}^{+a_u^k} du\, P_n(u) = 0\ , n = 1,\ldots,N \tag{6g}$$

By substituting Equation (6) into Equation (5f), expressions for the surface-average currents over the node surface at $u = \pm a_u^k$ are obtained as:

$$\bar{J}_{gu}^k(\pm a_u^k) = -\frac{D_g^k}{2a_u^k}\left(c_{gu1}^k \pm 3c_{gu2}^k + \frac{1}{2}c_{gu3}^k \pm \frac{1}{5}c_{gu4}^k\right) \tag{7}$$

Similarly, upon substitution of Equation (6) into Equation (5c), the transverse-integrated source can be approximated by polynomials of the following form:

$$Q_{gu}^k(u) = \bar{Q}_g^k + \sum_{n=1}^{4} q_{gun}^k\, P_n(u) \tag{8a}$$

where $q_{gun}^k$ are the expansion coefficients:

$$q_{gun}^k = \frac{\chi_g^k}{\lambda}\sum_{g'=1}^{G}(\nu\Sigma_f)_{g'}^k\, a_{gun}^k + \sum_{\substack{g'=1 \\ g'\neq g}}^{G}\Sigma_{gg'}^k\, a_{gun}^k \tag{8b}$$

### 3.3 Weighted-Residual Procedure

Setting $u = \pm a_u^k$ in the Equation (6), the two lower-order coefficients of the quartic polynomial for the transverse-integrated flux can easily be expressed in terms of the nodal volume-average flux and transverse-integrated flux on the surface as:

$$c_{gu1}^k = \phi_{gu}^k(+a_u^k) - \phi_{gu}^k(-a_u^k)$$
$$c_{gu2}^k = \phi_{gu}^k(+a_u^k) + \phi_{gu}^k(-a_u^k) - 2\bar{\phi}_g^k$$

To obtain two higher-order coefficients of the quartic polynomial for the transverse-integrated flux, a weighted-residual procedure is applied to Equation (5a), and yields the additional moment equations needed:

$$\int_{-\frac{1}{2}}^{+\frac{1}{2}} d\xi\, \omega_n(u)\left[\frac{\partial}{\partial u}J_{gu}^k(u) + \Sigma_{rg}^k\phi_{gu}^k(u)\right] = \int_{-\frac{1}{2}}^{+\frac{1}{2}} d\xi\, \omega_n(u)\left[Q_{gu}^k(u) - \frac{1}{2a_v^k}L_{gv}^k(u) - \frac{1}{2a_w^k}L_{gw}^k(u)\right] \tag{9}$$
$$u = x,y,z; g = 1,\ldots,G; k = 1,\ldots,K$$

The nodal balance Equation (2a), recovered using $\omega_0(u) = 1$, is regarded as the zeroth moment equation.

The first and second moment equations are obtained by weighting with $\omega_1(u)$ and $\omega_2(u)$, where these functions are specified using either moments weighting:

$$\omega_1(u) = P_1(u), \quad \omega_2(u) = P_2(u)$$

or Galerkin weighting:

$$\omega_1(u) = P_3(u), \quad \omega_2(u) = P_4(u)$$

Numerical studies[2] have shown that moments weighting yields superior accuracy, relative to Galerkin weighting in NEM approximation.

### 3.4 Transverse-Leakage Approximation

To solve Equation (9), the transverse leakage terms appearing on the right-hand side of the equation must be approximated as well. The "flat" approximation and the "quadratic" approximation are the two most-commonly used approximations. The approximation used in NEM is the "quadratic" transverse leakage approximation. For example, the average u-directed transverse leakage along v is given by:

$$L_{gv}^k(u) = \overline{L}_{gv}^k + \sum_{n=1}^{2} l_{gvn}^k P_n(u) \qquad (10a)$$
$$u = x, y, z; g = 1, \ldots, G; k = 1, \ldots, K$$

where the nodal surface-average, *v*-directed, net leakage in node *k* is expressed as:

$$\overline{L}_{gv}^k = \frac{1}{2a_u^k} \int_{-a_u^k}^{a_u^k} du L_{gv}^k(u) = J_{gv}^k(+a_v^k) - J_{gv}^k(-a_v^k) \qquad (10b)$$

and, the expansion coefficients $l_{gvn}^k$ can be obtained as the following in terms of the nodal surface-average, *v*-directed leakage in three adjacent nodes (*i.e.* node *k-1, k* and *k+1*) so as to preserve the node-average leakage in these three nodes:

$$l_{gv1}^k = \overline{L}_{gv}^k$$

$$l_{gv2}^k = \frac{a_u^k}{h^k}\left\{(2a_u^{k-1} + a_u^k)(a_u^k + a_u^{k-1})(\overline{L}_{gv}^{k+1} - \overline{L}_{gv}^k) + (a_u^k + a_u^{k+1})(a_u^k + 2a_u^{k+1})(\overline{L}_{gv}^k - \overline{L}_{gv}^{k-1})\right\}$$

$$l_{gv3}^k = \frac{(a_u^k)^2}{h^k}\left\{(a_u^{k-1} + a_u^k)(\overline{L}_{gv}^{k+1} - \overline{L}_{gv}^k) - (a_u^k + a_u^{k+1})(\overline{L}_{gv}^k - \overline{L}_{gv}^{k-1})\right\}$$

where

$$h^k = (a_u^{k-1} + a_u^k)(a_u^k + a_u^{k-1})(a_u^{k-1} + a_u^k + a_u^{k+1})$$

The classical approach to the above-derived NEM formulation is the response-matrix technique, in which the surface-average partial currents (incoming and outgoing currents) are used as the unknowns and are solved iteratively. This approach has been demonstrated to be quite successful and has been adopted in the

Siemens PANBOX code and Westinghouse ANC code. However, to minimize memory requirements, and especially to facilitate the capability of applying the NEM to a current commercial FDM code such as RFSP, an alternative non-linear iterative approach to NEM is proposed in this study. This technique was originally developed by Smith, successfully implemented in the Studsvik Scandpower QPANDA and SIMULATE-3 codes, and subsequently refined and extended in the FORMOSA and NESTLE codes. To illustrate this approach, we start from the NEM two-node problem.

## 4. NEM TWO-NODE PROBLEM

Assuming the node volume-average fluxes are known from a previous FDM solution, then, the total number of unknown expansion coefficients per node per energy in each direction is 4G ($c^k_{gun}$, $n = 1,\ldots,4$, $g=1,\ldots G$, $u = x, y, z$), yields 8G unknowns for the following two adjacent nodes. The 8G constraint equations required to calculate these unknowns, listed in Table 1, are obtained as follows,

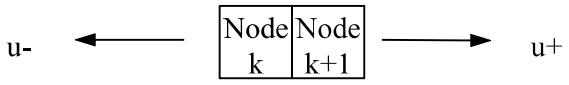


Zeroth Moment Equation

We begin with the substitution of Equation (7) into the nodal balance equation, Equation (2a), for node k, we yield the zeroth moment equations:

$$-6D^k_g c^k_{gu2} - 0.4D^k_g c^k_{gu4} = \left[\left(\overline{Q}^k_g - \frac{1}{2a^k_v}\overline{L}^k_{gv} - \frac{1}{2a^k_w}\overline{L}^k_{gw}\right) - \Sigma^k_{rg}\overline{\phi}^k_g\right]\left(2a^k_u\right)^2 \qquad (11)$$
$$u = x, y, z; g = 1,\ldots,G; k = 1,\ldots,K$$

First Moment Equation

Similarly, substitution of Equations (6), (7), (8), and (10) into the moment Equation (9) using $\omega_1(u) = P_1(u)$, yields the first moment equations:

$$10\Sigma^k_{rg} c^k_{gu1} - \left(\frac{60D^k_g}{\left(2a^k_u\right)^2} + \Sigma^k_{rg}\right)c^k_{gu3} = 10q^k_{gu1} - q^k_{gu3} - 10\left(\frac{l^k_{gv1}}{2a^g_v} + \frac{l^k_{gw1}}{2a^g_w}\right) \qquad (12a)$$
$$u, v, w = x, y, z;\ u \neq v \neq w;\ g = 1,\ldots,G;\ k = 1,\ldots,K$$

For two-group approximation, the above equation can be written as:

$$-10\left(\Sigma_{r1}^{k}-\frac{1}{\lambda}\nu\Sigma_{f1}^{k}\right)c_{1u1}^{k}+10\frac{1}{\lambda}\nu\Sigma_{f2}^{k}c_{2u1}^{k}+\left[\frac{60D_{1}^{k}}{\left(2a_{u}^{k}\right)^{2}}+\left(\Sigma_{rg}^{k}-\frac{1}{\lambda}\nu\Sigma_{f1}^{k}\right)\right]c_{1u3}^{k}$$
$$-\frac{1}{\lambda}\nu\Sigma_{f2}^{k}c_{2u3}^{k}=10\left(\frac{l_{1v1}^{k}}{2a_{v}^{k}}+\frac{l_{1w1}^{k}}{2a_{w}^{k}}\right) \tag{12b}$$

$$10\Sigma_{21}^{k}c_{1u1}^{k}-10\Sigma_{r2}^{k}c_{2u1}^{k}-\Sigma_{21}^{k}c_{1u3}^{k}+\left[\frac{60D_{2}^{k}}{\left(2a_{u}^{k}\right)^{2}}+\Sigma_{r2}^{k}\right]c_{2u3}^{k}=10\left(\frac{l_{2v1}^{k}}{2a_{v}^{k}}+\frac{l_{2w1}^{k}}{2a_{w}^{k}}\right) \tag{12c}$$

Second Moment Equation

Similarly, substitution of Equations (6), (7), (8), and (10) into the moment Equation (9) using $\omega_2(u)=P_2(u)$, yields the second moment equations:

$$35\Sigma_{rg}^{k}c_{gu2}^{k}-\left(\frac{140D_{g}^{k}}{\left(2a_{u}^{k}\right)^{2}}+\Sigma_{rg}^{k}\right)c_{gu4}^{k}=35q_{gu2}^{k}-q_{gu4}^{k}-35\left(\frac{l_{gv2}^{k}}{2a_{v}^{g}}+\frac{l_{gw2}^{k}}{2a_{w}^{g}}\right) \tag{13a}$$
$$u,v,w=x,y,z;\ u\neq v\neq w;\ g=1,\ldots,G;\ k=1,\ldots,K$$

For the two-group approximation, the above equation can be written as:

$$-35\left(\Sigma_{r1}^{k}-\frac{1}{\lambda}\nu\Sigma_{f1}^{k}\right)c_{1u2}^{k}+35\frac{1}{\lambda}\nu\Sigma_{f2}^{k}c_{2u2}^{k}+\left[\frac{140D_{1}^{k}}{\left(2a_{u}^{k}\right)^{2}}+\left(\Sigma_{r1}^{k}-\frac{1}{\lambda}\nu\Sigma_{f1}^{k}\right)\right]c_{1u4}^{k}$$
$$-\frac{1}{\lambda}\nu\Sigma_{f2}^{k}c_{2u4}^{k}=35\left(\frac{l_{1v2}^{k}}{2a_{v}^{k}}+\frac{l_{1w2}^{k}}{2a_{w}^{k}}\right) \tag{13b}$$

$$35\Sigma_{21}^{k}c_{1u2}^{k}-35\Sigma_{r2}^{k}c_{2u2}^{k}-\Sigma_{21}^{k}c_{1u4}^{k}+\left[\frac{180D_{g}^{k}}{\left(2a_{u}^{k}\right)^{2}}+\Sigma_{r2}^{k}\right]c_{2u4}^{k}=35\left(\frac{l_{2v2}^{k}}{2a_{v}^{k}}+\frac{l_{2w2}^{k}}{2a_{w}^{k}}\right) \tag{13c}$$

Continuity of the Surface-Average Currents

Based on the continuity of surface-average current constraints of the two adjacent nodes *k* and *k+1*:

$$\bar{J}_{gu}^{k}(+a_{u}^{k})=\bar{J}_{gu}^{k+1}(-a_{u}^{k+1})$$

we obtain the following equation by using Equation (7):

$$3\left(2a_u^{k+1}\right)D_g^k c_{gu2}^k + 0.2\left(2a_u^{k+1}\right)D_g^k c_{gu4}^k + 3\left(2a_u^k\right)D_g^{k+1} c_{gu2}^{k+1} + 0.2\left(2a_u^k\right)D_g^{k+1} c_{gu4}^{k+1}$$
$$- 2a_u^{k+1} D_g^k c_{gu1}^k + a_u^{k+1} D_g^k c_{gu3}^k - 2a_u^k D_g^{k+1} c_{gu1}^{k+1} - a_u^k D_g^{k+1} c_{gu3}^{k+1} = 0 \qquad (14)$$
$$u = x, y, z; g = 1, \ldots, G; k = 1, \ldots, K$$

Discontinuity of the Surface-Average Fluxes

Finally, the discontinuity of surface-average flux constraints is imposed on the two adjacent nodes as:

$$f_{gu+}^k \phi_{gu}^k (+a_u^k) = f_{gu-}^{k+1} \phi_{gu}^{k+1} (-a_u^{k+1}) \qquad (15)$$

The assembly homogenization techniques for LWR analysis can introduce significant error when flux- and volume-weighted macroscopic cross sections are used in homogenized nodal reactor models. This error can be significant (10% to 15% in assembly powers)[11][12] for LWR fuel assemblies that have lumped absorbers, such as control rods or burnable absorbers. The discontinuity factors $f_{gu+}^k$ [11][12], introduced to eliminate most of these errors in LWR applications, can be obtained from lattice physics calculations by using the following definition:

$$f_{gu\pm}^k = \frac{\phi_{gu}^{k,het}(\pm a_u^k)}{\phi_{gu}^k(\pm a_u^k)} \qquad (16)$$

where, $\phi_{gu}^{k,het}(\pm a_u^k)$ is the surface-average flux obtained from the reference heterogeneous solution, and $\phi_{gu}^k(\pm a_u^k)$ is the surface-average flux implied by the solution to Equation (1) for node $k$. Substituting Equation (6) to Equation (15), yields the following equation:

$$\frac{1}{2} f_{gu+}^k c_{gu2}^k - \frac{1}{2} f_{gu-}^{k+1} c_{gu2}^{k+1} + \frac{1}{2} f_{gu+}^k c_{gu1}^k + \frac{1}{2} f_{gu-}^{k+1} c_{gu1}^{k+1} = f_{gu-}^{k+1} \bar{\phi}_g^{k+1} - f_{gu+}^k \bar{\phi}_g^k \qquad (17)$$
$$u = x, y, z; g = 1, \ldots, G; k = 1, \ldots, K$$

It should be mentioned that, although the use of the discontinuity factors is quite common for LWR reactors, it is not an important issue for CANDU reactors with the cluster-type fuel lattice design. The discontinuity factors, introduced in our nodal formulation for completeness, will be set to 1.0 for our CANDU analysis.

Closed Equation

Applying Equations (11), (12), (13), (14) and (17) to two adjacent nodes for each energy group, a closed 8G x 8G system of equations for the solution of the NEM two-node problem is derived in the following form,

$$A\vec{x} = B \qquad (18)$$

where $\vec{x}$ is the vector of unknown 8G expansion coefficients for two adjacent nodes, and the coefficient matrix $A$ and the right-hand-side $B$ are known from the last iteration.

With the expansion coefficients known after solving this 8G x 8G matrix system, the NEM currents can be calculated for each nodal surface. Note that the matrix A is not a diagonal-dominant matrix, and the solution of this matrix system has an important effect on the calculation accuracy. Further investigation should be made during the practical application of this method to CANDU analysis.

## 5. NON-LINEAR ITERATIVE STRATEGY

### 5.1 Updating of FDM Coupling Coefficients

Solutions of Equation (8) of the two-node problems provide NEM-evaluated values of the currents on all surfaces. To correct the FDM approximation of the surface-average current, the FDM coupling coefficients can be updated by the following approach to force FDM and NEM interface currents to match:

$$\bar{J}_{gu}^{k,FDM}(a_u^k) = -\frac{1}{2a_v^k\, 2a_w^k}\left\{d_{gu+}^{k,FDM}\left[\bar{\phi}_g^{k+1} - \bar{\phi}_g^{k}\right] - d_{gu+}^{k,NEM}\left[\bar{\phi}_g^{k+1} + \bar{\phi}_g^{k}\right]\right\} = \bar{J}_{gu}^{k,NEM}(a_u^k) \qquad (19)$$

$$u,v,w = x,y,z;\ u \neq v \neq w;\ g = 1,\ldots,G;\ k = 1,\ldots,K$$

where the first term on the right-hand side is the nominal FDM approximation as shown in Equation (3), and the second term on the right-hand side represents the non-linear NEM correction applied to the FDM approximation. Assuming the NEM-predicted surface-average currents, $\bar{J}_{gu}^{k,NEM}(a_u^k)$, are known, the coefficients of the NEM correction term, $d_{gu+}^{k,NEM}$, can be easily updated.

Substitution of Equation (19) into the nodal balance equation, Equation (2), results in a new FDM neutron-diffusion equation:

$$\sum_{n=1}^{6} \tilde{d}_g^{0n}\left(\bar{\phi}_g^0 - \bar{\phi}_g^n\right) + \Sigma_{r,g}^0\, \bar{\phi}_g^0\, V^0 = \bar{Q}_g^0\, V^0 \qquad (20)$$

Equation (20) is of the same form as Equation (4) except for the NEM-corrected coupling coefficients $\tilde{d}_g^{0n}$, which are non-linearly updated based on NEM-derived currents. Repeating this non-linear iterative procedure several times, the FDM neutron-diffusion equation, Equation (20), will yield the same node-average flux distribution and fundamental mode eigenvalue as computed by NEM.

### 5.2 Iteration Procedures

The overall iteration strategy of the non-linear iterative NEM strategy discussed here has the following complicated nested three-level structure:

1) coupling coefficient iteration

2) fission source iteration
3) nodal flux iteration

The coupling coefficient iteration arises primarily because of the NEM correction to the FDM approximation. Both fission-source and flux iteration are standard iteration procedures used in the FDM. The basic procedure for this non-linear iterative approach is as follows:

1) Compute initial FDM coupling coefficients $d_g^{0n,FDM}$ based upon the FDM approximation (Equation (3)).
2) Set NEM-corrected coupling coefficients $\tilde{d}_g^{0n}$ in Equation (20) equal to the initial FDM coupling coefficients calculated in step 1.
3) Solve the coarse-mesh FDM neutron-diffusion Equation (20) to get nodal volume-average flux distributions. Check for convergence of both fission source and nodal flux.
4) Update the coefficient matrix $A$ and the right-hand-side $B$ in Equation (18), and then solve NEM two-node problems to provide the NEM-evaluated surface-average current for each nodal surface.
5) Update NEM-corrected coupling coefficients $\tilde{d}_g^{0n}$ in Equation (20) to force the FDM- and NEM-derived surface-average currents to agree.
6) Return to step 3 with the updated coupling coefficients until convergence is reached.

Numerically, the NEM currents and coupling-coefficients corrections are non-linearly updated in an outer-nested iterative fashion. For the LWR application, the process has proven to be a convergent technique that forces the FDM equations to yield nearly the same node-average flux distribution and fundamental-mode eigenvalue as computed by NEM.

## 6. PRELIMINARY NUMERICAL TESTS

To verify the formulation and iteration strategy described in this paper, a two-group two-dimensional steady-state non-linear iterative NEM formulation was programmed and implemented into a simple FDM code. The new code named NINEM has the capability of using either NEM or the FDM formulation. A series of 2-D benchmark problems have been tested. The coarse-mesh NEM results were comparable to both coarse-mesh and fine-mesh FDM calculations using one code (NINEM) on the same UNIX workstation.

### Two-Dimensional BIBLIS PWR Problem[2][13]

This is a realistic commercial operating PWR problem and the base mesh spacing is 23.1226 cm per assembly. The large assembly size and the checkerboard fuel-assembly loading pattern make the problem hard to solve accurately. Figure 2 compares the normalized assembly-average power densities from the coarse-mesh (1 x 1 and 2 x 2 per assembly) NEM calculation, the coarse mesh (2 x 2 per assembly) and the fine-mesh (15 x 15 per assembly) FDM calculations. Compared with the fine-mesh (15 x 15 per assembly) FDM results, the coarse-mesh (2 x 2 per assembly) FDM yields a maximum error in the assembly-average power densities of about 23% at the core periphery region, and is not considered reliable for PWR analysis. However, the coarse-mesh NEM results are in very good agreement with the fine-mesh (15 x 15 per assembly) FDM results, with maximum errors in the assembly-average power densities of about 1.4% and 0.2% for NEM (1 x 1) and NEM (2 x 2), respectively.

Two-Dimensional EPRI-9 Benchmark Problem[14]

This is a simplified 2-D 2-group benchmark problem used to validate the capability of applying the discontinuity factors in our nodal code. The base mesh spacing is 20 cm per assembly. Figure 3 compares the normalized assembly-average power densities from the coarse-mesh (1 x 1 per assembly) NEM calculation, the coarse-mesh (1 x 1 per assembly) and the fine-mesh (20 x 20 per assembly) FDM calculations, in which discontinuity factors were not considered. Compared with the fine-mesh (20 x 20 per assembly) FDM results, the coarse-mesh (1 x 1 per assembly) FDM yields a maximum error in the assembly-average power densities of about 15%. However, the coarse-mesh (1 x 1 per assembly) NEM results show very good agreement with the fine-mesh (20 x 20 per assembly) FDM results, the maximum error in the assembly-average power densities is only 0.9%.

Figure 4 shows the normalized assembly-average power densities of the coarse mesh (1 x 1 and 2 x 2 per assembly) NEM and reference solution[14], in which discontinuity factors were considered. Once again, we note that the coarse-mesh NEM results show very good agreement with the reference solution.

Two-Dimensional CANDU Benchmark Problem[15]

This is a simplified 2-D CANDU core with only two fuel regions (inner and outer fuel regions) in the core, surrounded by a heavy-water reflector, as shown in the Figure 5. A non-uniform 32 x 32 mesh consisting of mesh spacings of 15 cm and 30 cm was used as the base mesh. Figure 6 compares the normalized assembly-average power densities from the coarse-mesh (1 x 1 sub-mesh) NEM calculation, the coarse-mesh (1 x 1 and 2 x 2 sub-mesh) and the fine-mesh (8 x 8 sub-mesh) FDM calculations.

The coarse-mesh (1 x 1 sub-mesh) FDM-derived eigenvalues agree well (0.981183 vs. 0.981184) between our NINEM calculation and the reference CERKIN calculation provided in Reference 15. To compare the accuracy of coarse-mesh FDM and NEM results, a fine-mesh (8 x 8 sub-mesh) FDM calculation was performed with our NINEM code and used as the new "reference" shown in the first row in each box of Figure 6.

Compared with the reference fine-mesh (8 x 8 sub-mesh) FDM results, the coarse-mesh FDM calculations show good agreement in the assembly-average power densities for the core interior region, with maximum errors in the assembly-average power densities of about 1.4% and 0.4% (located near the boundary of the inner and outer regions) for FDM (1 x 1) and FDM (2 x 2) respectively. However, for the core periphery region (the region close to the reflector), the maximum errors in the assembly-average power densities reach about 5.9% and 2.4% for FDM (1 x 1) and FDM (2 x 2), respectively. Such errors can be avoided by using the nodal method. As shown in Figure 6, the coarse-mesh (1 x 1 per assembly) NEM results show very good agreement with the fine-mesh (8 x 8 sub-mesh) FDM results, with a maximum error in the assembly-average power densities, located in the core periphery region as well, of about 0.8%.

The last row in each box of Figure 6 shows the NEM (1 x 1) results with the "flat" transverse leakage approximation. Clearly the NEM (1 x 1) results with the "flat" transverse leakage approximation are as accurate as the NEM (1 x 1) results with the "quadratic" transverse leakage approximation. This implies that the "flat" transverse leakage approximation, as used in Reference 1 for 3-D CANDU transient scenario, would be an adequate approximation for CANDU analysis.

The CANDU benchmark problem shown here is quite simple; it is anticipated that the higher accuracy of the nodal method compared to FDM method would be obtained for a realistic CANDU problem having a more complex flux shape.

## 7. CONCLUSIONS

In this paper, the steady-state nodal diffusion formulation of the non-linear iterative nodal expansion method (NEM) was derived independently and illustrated in detail. A simple 2-D two-group diffusion code with the capability of both finite-difference method (FDM) and NEM techniques has also been developed. Preliminary numerical tests show that the formulation derived in the paper is correct, and the NEM always shows superior accuracy over the FDM for a given mesh design, even for CANDU analysis. The coarse-mesh (about a 20-cm mesh spacing for PWRs and a 30-cm mesh spacing for CANDU reactors) NEM results are as accurate as the fine-mesh (about a 1- to 1.5-cm mesh spacing for PWRs, and a 5-cm mesh spacing for CANDU reactors) FDM results for both PWR and CANDU analysis.

It should be noted that, even though the nodal formulation we derived in this paper is for the solution of the 3-D multi-group steady-state diffusion equation, the code we developed is very preliminary and is suited for formulation-testing purposes only. The FDM code we selected is a simple independent academic one without acceleration technique, and was limited to 2-D geometry with the constrained boundary conditions. Also the 8G x 8G matrix solver and the non-linear iteration procedure need to be refined and widely verified. Possible idea for further investigation are extension of the code to 3-D geometry and application of the nodal method to a 3-D CANDU benchmark problem. If this method is proven to be efficient for CANDU analysis, it should be practical to implement it in RFSP in the future.

**Acknowledgments**: Special thanks go to J.M. Noh of Korea Atomic Energy Research Institute (KAERI) for the useful discussions on the NEM two-node problem. J. Mao of École Polytechnique de Montréal is also acknowledged for her assistance with CANDU benchmarking. Part of this work was funded by KAERI.

## REFERENCES

1. J. Mao and J. Koclas, "The Analytic Nodal Method for CANDU Reactor Three-Dimensional Space-Time Kinetic Calculations", 21st Canadian Nuclear Society Annual Conference, Toronto, June 11-14, 2000.
2. H. Finnemann, F. Bennewitz and M.R. Wagner, "Interface Current for Multidimensional Reactor Calculations" Atomkemenergie, 30, 123, 1977.
3. Y.S. Liu, et al., "ANC - Westinghouse Advanced Nodal Computer Code", WCAP-10966-A, Dec. 1986.
4. K.S. Smith, "Nodal Method Storage Reduction by Non-linear Iteration" Trans. Am. Nucl. Soc., 44, 265, 1983.
5. K.S. Smith, D.M. Ver Planck and M. Edenius, "QPANDA: An Advanced Nodal Method for LWR Analysis" Trans. Am. Nucl. Soc., 50, 532, 1985.
6. M. Edenius, K.S. Smith and D.M. Ver Planck, "Recent Developments in the MICBURN/CASMO/SIMULATE LWR Analysis Package", ANS Topical Meeting on Advances in Fuel Management, Pinehurst, NC, 1986.
7. P.R. Engrand, G.I. Maldonado, R.M. Al-Chalabi and P.J. Turinsky, "Non-linear Iterative Strategy for

NEM: Refinement and Extension", Trans. Am. Nucl. Soc., 65, 221, 1992.
8. P.J. Turinsky, "NESTLE, A Nodal Kinetics Code", Trans. Am. Nucl. Soc., Vol. 68, pp 432, 1993.
9. B. Rouben, "Overview of Current RFSP-Code Capabilities for CANDU Core Analysis", Atomic Energy of Canada Limited Report, AECL Report, AECL-11407, 1996.
10. K.S. Smith, "An Analytical Nodal Method For Solving The Two-Group, Multi-Dimensional, Static And Transient Neutron Diffusion Equations", M.Sc. Thesis, Massachusetts Institute of Technology, 1979.
11. K. Koebke, " Advances in Homogenization and Dehomogenization", International Topical Meeting on Advances in Mathematical Methods for the Solution of Nuclear Engineering Problem, Vol. 2, Munich, 27-29 April, 1981.
12. K.S. Smith, "Assembly Homogenization Techniques for Light Water Reactor Analysis",Prog. Nucl. Energy, Vol. 17, No. 3, 1986.
13. W. Shen, Z. Xie and B. Yin, "The Green's Function Nodal Expansion Method for Light Water Reactor Diffusion Calculations",Nucl. Sci. Eng., 121, 1995.
14. H.S. Khalil, "The Application of Nodal Methods to PWR Analysis", Ph.D. Thesis, Dept. of Nucl. Eng., MIT, 1983.
15. National Energy Software Center, "Benchmark Problem Book", ANL-7416, 1985.

Table 1: 8G Constraints for NEM Two-Node Problem (8 Equations for Each Group)

| Node *k* | Node *k+1* |
|---|---|
| Zero Moment Equation | Zero Moment Equation |
| First Moment Equation | First Moment Equation |
| Second Moment Equation | Second Moment Equation |
| Current Continuity | |
| Flux Discontinuity | |

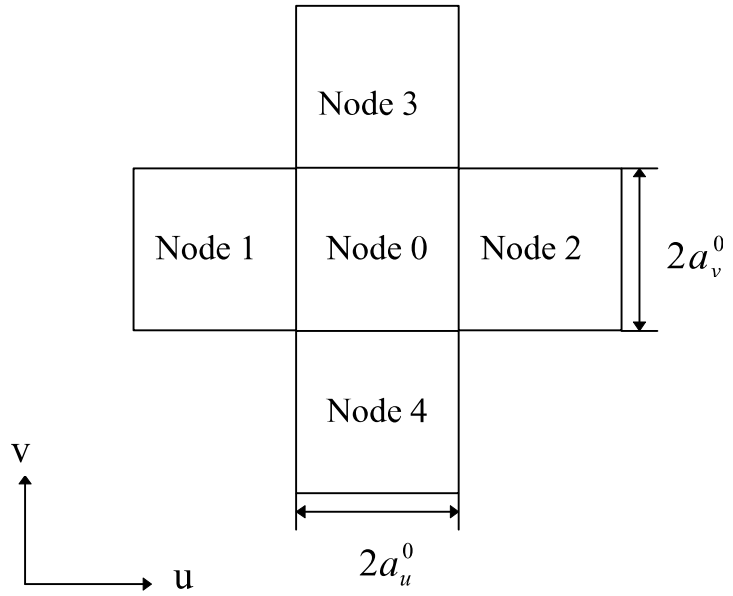


Figure 1: Schematic 2-D View of Typical Node Showing Nodes to which It Is Coupled

| | | | | | | | |
|---|---|---|---|---|---|---|---|
| 1.094 | 1.102 | 1.246 | 1.221 | 1.091 | 0.980 | 1.094 | 1.012 |
| 0.922 | 0.899 | 1.077 | 1.057 | 1.009 | 0.927 | 1.162 | 1.211 |
| 1.090 | 1.100 | 1.244 | 1.219 | 1.089 | 0.979 | 1.089 | 1.003 |
| 1.092 | 1.103 | 1.244 | 1.221 | 1.089 | 0.981 | 1.093 | 1.011 |
| | 1.121 | 1.134 | 1.227 | 1.067 | 1.033 | 1.071 | 0.968 |
| | 0.955 | 0.946 | 1.103 | 0.956 | 1.019 | 1.138 | 1.162 |
| | 1.120 | 1.131 | 1.226 | 1.064 | 1.032 | 1.068 | 0.958 |
| | 1.119 | 1.135 | 1.225 | 1.068 | 1.032 | 1.070 | 0.967 |
| | | 1.126 | 1.105 | 1.123 | 0.922 | 0.931 | 0.822 |
| | | 0.996 | 0.966 | 1.069 | 0.881 | 1.000 | 0.667 |
| | | 1.127 | 1.102 | 1.125 | 0.920 | 0.933 | 0.819 |
| | | 1.124 | 1.105 | 1.121 | 0.923 | 0.930 | 0.822 |
| | | | 1.164 | 1.038 | 0.952 | 0.763 | 0.544 |
| | | | 1.096 | 0.971 | 0.975 | 0.810 | **0.667*** |
| | | | 1.167 | 1.039 | 0.957 | 0.765 | 0.546 |
| | | | 1.163 | 1.039 | 0.951 | 0.764 | 0.545 |
| | | | | 1.124 | 0.992 | 0.873 | |
| | | | | 1.146 | 1.035 | 1.019 | |
| | | | | 1.131 | 1.000 | 0.883 | |
| | | | | 1.124 | 0.993 | **0.875** | |
| | | | | | 1.199 | 0.683 | -- FDM (15 x 15) K = 1.025129 |
| | | | | | 1.382 | 0.844 | -- FDM (2 x 2) K = 1.028479 |
| | | | | | **1.216** | 0.683 | -- NEM (1 x 1) K = 1.025210 |
| | | | | | 1.201 | 0.684 | -- NEM (2 x 2) K = 1.025102 |

*Note: The assembly-average power densities with the maximum calculation error are shown in bold characters,

Figure 2: Normalized Assembly-Average Power Densities for 2-D BIBLIS PWR Problem
(one eighth Symmetric Core Configuration)

| | | |
|---|---|---|
| 1.407 | 1.195 | 0.863 |
| 1.230 | 1.104 | 0.934 |
| 1.413 | 1.199 | 0.862 |
| 1.195 | 1.190 | 0.643 |
| 1.104 | 1.216 | **0.738*** |
| 1.199 | 1.191 | **0.637** |
| 0.863 | 0.643 | -- FDM (20 x 20) K = 0.927904 |
| 0.934 | 0.738 | -- FDM (1 x 1) K = 0.936029 |
| 0.862 | 0.637 | -- NEM (1 x 1) K = 0.927694 |

*Note: The assembly-average power densities with the maximum calculation error are shown in bold characters.

Figure 3: Normalized Assembly-Average Power Densities for the EPRI-9 Benchmark Problem (No Discontinuity Factors)

| | | |
|---|---|---|
| 1.449 | 1.224 | 0.847 |
| 1.446 | 1.220 | 0.849 |
| 1.224 | 1.204 | 0.603 |
| 1.220 | 1.204 | **0.606*** |
| 0.847 | 0.603 | -- Reference K = 0.926423 |
| 0.849 | 0.606 | -- NEM (1 x 1) K = 0.926536 |

*Note: The assembly-average power densities with the maximum calculation error are shown in bold characters.

Figure 4: Normalized Assembly-Average Power Densities for the EPRI-9 Benchmark Problem **(With Discontinuity Factors)**

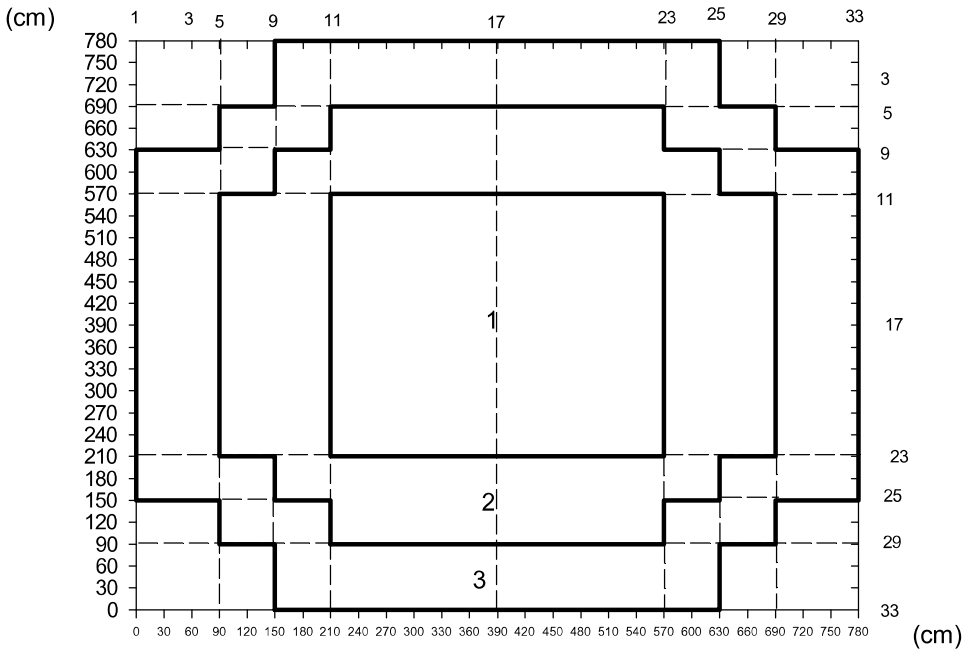


Note:

1. Zero flux boundary conditions on external surfaces
2. A non-uniform 32 x 32 meshe consisting of mesh spacings of 15 cm and 30 cm was used as the base meshes.
3. There are two fuel regions (regions 1 and 2) in the core, surrounded by a heavy-water reflector (region 3)

Figure 5: Geometry Description of 2-D CANDU Benchmark Problem

| | | | | | | | | | | | |
|---|---|---|---|---|---|---|---|---|---|---|---|
| 1.199 | 1.196 | 1.191 | 1.186 | 1.182 | 1.183 | 1.191 | 1.114 | 1.007 | 0.915 | 0.819 | 0.760 |
| 1.205 | 1.202 | 1.196 | 1.190 | 1.185 | 1.184 | 1.207 | 1.127 | 1.008 | 0.914 | 0.813 | 0.734 |
| 1.203 | 1.200 | 1.195 | 1.189 | 1.184 | 1.184 | 1.196 | 1.118 | 1.008 | 0.915 | 0.817 | 0.752 |
| 1.197 | 1.194 | 1.189 | 1.184 | 1.181 | **1.181** | 1.190 | 1.113 | 1.007 | 0.915 | 0.819 | 0.760 |
| 1.196 | 1.193 | 1.189 | 1.184 | 1.180 | 1.182 | 1.191 | 1.115 | 1.008 | 0.917 | 0.820 | 0.762 |
| | 1.193 | 1.186 | 1.179 | 1.172 | 1.169 | 1.174 | 1.095 | 0.989 | 0.897 | 0.802 | 0.743 |
| | 1.198 | 1.191 | 1.182 | 1.175 | 1.170 | **1.190** | 1.108 | 0.989 | 0.896 | 0.796 | 0.718 |
| | 1.196 | 1.189 | 1.181 | 1.174 | 1.171 | **1.179** | 1.099 | 0.989 | 0.897 | 0.800 | 0.736 |
| | 1.191 | 1.184 | 1.177 | 1.171 | 1.168 | 1.173 | 1.095 | 0.988 | 0.897 | 0.802 | 0.744 |
| | 1.190 | 1.184 | **1.176** | 1.170 | 1.169 | 1.174 | 1.096 | 0.990 | 0.899 | 0.803 | 0.745 |
| | | 1.177 | 1.165 | 1.152 | 1.143 | 1.141 | 1.058 | 0.950 | 0.860 | 0.767 | 0.709 |
| | | 1.181 | 1.168 | 1.154 | 1.143 | 1.155 | 1.068 | 0.950 | 0.859 | 0.761 | 0.685 |
| | | 1.180 | 1.167 | 1.154 | 1.144 | 1.145 | 1.060 | 0.950 | 0.860 | 0.765 | 0.702 |
| | | 1.175 | 1.163 | 1.151 | 1.142 | 1.140 | 1.057 | 0.951 | 0.861 | 0.767 | 0.710 |
| | | 1.175 | 1.163 | 1.151 | 1.142 | 1.141 | 1.059 | 0.952 | 0.862 | 0.769 | 0.711 |
| | | | 1.146 | 1.124 | 1.104 | 1.090 | 0.999 | 0.891 | 0.803 | 0.712 | 0.656 |
| | | | 1.148 | 1.125 | 1.103 | 1.101 | 1.008 | 0.890 | 0.800 | 0.706 | 0.633 |
| | | | 1.148 | 1.126 | 1.104 | 1.093 | 1.001 | 0.890 | 0.801 | 0.710 | 0.648 |
| | | | 1.145 | 1.123 | 1.103 | 1.090 | 1.000 | 0.892 | 0.803 | 0.713 | 0.657 |
| | | | 1.144 | 1.123 | 1.103 | 1.090 | 1.001 | 0.893 | 0.804 | 0.714 | 0.658 |
| | | | | 1.090 | 1.053 | 1.021 | 0.919 | 0.809 | 0.722 | 0.635 | 0.579 |
| | | | | 1.089 | 1.051 | 1.030 | 0.925 | 0.806 | 0.718 | 0.628 | 0.558 |
| | | | | 1.091 | 1.053 | 1.023 | 0.920 | 0.807 | 0.720 | 0.632 | 0.572 |
| | | | | 1.090 | 1.053 | 1.022 | 0.920 | 0.810 | 0.723 | 0.636 | 0.581 |
| | | | | 1.089 | 1.053 | 1.022 | 0.921 | 0.810 | 0.723 | 0.636 | 0.581 |
| | | | | | 0.994 | 0.935 | 0.822 | 0.728 | 0.647 | 0.558 | 0.494 |
| | | | | | 0.990 | 0.940 | 0.818 | 0.708 | 0.622 | 0.534 | **0.465*** |
| | | | | | 0.993 | 0.935 | 0.819 | 0.718 | 0.635 | 0.547 | **0.482** |
| | | | | | 0.995 | 0.936 | 0.824 | 0.732 | 0.651 | 0.563 | **0.498** |
| | | | | | 0.994 | 0.936 | 0.824 | 0.729 | 0.648 | 0.561 | **0.497** |
| | | | | | | 0.827 | 0.720 | | | | |
| | | | | | | 0.830 | 0.704 | | | | |
| | | | | | | 0.827 | 0.713 | | | | |
| | | | | | | 0.830 | 0.723 | | | | |
| | | | | | | 0.826 | 0.719 | | | | |
| | | | | | | | 0.591 | -- FDM (8 x 8) K = 0.981368 | | | |
| | | | | | | | 0.561 | -- FDM (1 x 1) K = 0.981193 | | | |
| | | | | | | | 0.579 | -- FDM (2 x 2) K = 0.981281 | | | |
| | | | | | | | 0.596 | -- NEM (1 x 1) K = 0.981415 | | | |
| | | | | | | | 0.593 | -- NEM (1 x 1) K = 0.981416 (Flat Leakage) | | | |

*Note: The assembly-average power densities with the maximum calculation errors in the core interior and periphery regions are shown in bold characters.

Figure 6: Normalized Assembly-Average Power Densities for 2-D CANDU Benchmark Problem
(one eighth Symmetric Core Configuration)